



UNIVERSITY OF LEEDS

This is a repository copy of *Spatial period-multiplying instabilities of hexagonal Faraday waves* .

White Rose Research Online URL for this paper:  
<http://eprints.whiterose.ac.uk/992/>

---

**Article:**

Tse, D.P., Rucklidge, A.M., Hoyle, R.B. et al. (1 more author) (2000) Spatial period-multiplying instabilities of hexagonal Faraday waves. *Physica D: Nonlinear Phenomena*, 146 (1-4). pp. 367-387. ISSN 0167-2789

[https://doi.org/10.1016/S0167-2789\(00\)00124-X](https://doi.org/10.1016/S0167-2789(00)00124-X)

---

**Reuse**

See Attached

**Takedown**

If you consider content in White Rose Research Online to be in breach of UK law, please notify us by emailing [eprints@whiterose.ac.uk](mailto:eprints@whiterose.ac.uk) including the URL of the record and the reason for the withdrawal request.



[eprints@whiterose.ac.uk](mailto:eprints@whiterose.ac.uk)  
<https://eprints.whiterose.ac.uk/>



White Rose  
university consortium  
Universities of Leeds, Sheffield & York

## White Rose Consortium ePrints Repository

<http://eprints.whiterose.ac.uk/>

This is an author produced version of a paper published in **Physica D: Nonlinear Phenomena**. This paper has been peer-reviewed but does not include final publisher proof-corrections or journal pagination.

White Rose Repository URL for this paper:  
<http://eprints.whiterose.ac.uk/archive/00000992/>

---

### Citation for the published paper

Tse, D.P. and Rucklidge, A.M. and Hoyle, R.B. and Silber, M. (2000) *Spatial period-multiplying instabilities of hexagonal Faraday waves*. Physica D: Nonlinear Phenomena, 146 (1-4). pp. 367-387.

### Citation for this paper

To refer to the repository paper, the following format may be used:

Tse, D.P. and Rucklidge, A.M. and Hoyle, R.B. and Silber, M. (2000) *Spatial period-multiplying instabilities of hexagonal Faraday waves*.

Author manuscript available at: <http://eprints.whiterose.ac.uk/archive/00000992/>  
[Accessed: *date*].

Published in final edited form as:

Tse, D.P. and Rucklidge, A.M. and Hoyle, R.B. and Silber, M. (2000) *Spatial period-multiplying instabilities of hexagonal Faraday waves*. Physica D: Nonlinear Phenomena, 146 (1-4). pp. 367-387.

# Spatial period-multiplying instabilities of hexagonal Faraday waves

D.P. Tse<sup>1</sup>, A.M. Rucklidge<sup>2</sup>, R.B. Hoyle

*Department of Applied Mathematics and Theoretical Physics,  
University of Cambridge, Silver Street, Cambridge CB3 9EW, UK*

and

M. Silber<sup>3</sup>

*Department of Engineering Sciences and Applied Mathematics,  
Northwestern University, Evanston, IL 60208 USA*

---

## Abstract

A recent Faraday wave experiment with two-frequency forcing reports two types of ‘superlattice’ patterns that display periodic spatial structures having two separate scales [1]. These patterns both arise as secondary states once the primary hexagonal pattern becomes unstable. In one of these patterns (so-called ‘superlattice-two’) the original hexagonal symmetry is broken in a subharmonic instability to form a striped pattern with a spatial scale increased by a factor of  $2\sqrt{3}$  from the original scale of the hexagons. In contrast, the time-averaged pattern is periodic on a hexagonal lattice with an intermediate spatial scale ( $\sqrt{3}$  larger than the original scale) and apparently has  $60^\circ$  rotation symmetry. We present a symmetry-based approach to the analysis of this bifurcation. Taking as our starting point only the observed instantaneous symmetry of the superlattice-two pattern presented in [1] and the subharmonic nature of the secondary instability, we show (a) that a pattern with the same instantaneous symmetries as the superlattice-two pattern can bifurcate stably from standing hexagons; (b) that the pattern has a spatio-temporal symmetry not reported in [1]; and (c) that this spatio-temporal symmetry accounts for the intermediate spatial scale and hexagonal periodicity of the time-averaged pattern, but not for the apparent  $60^\circ$  rotation symmetry. The approach is based on general techniques that are readily applied to other secondary instabilities of symmetric patterns, and does not rely on the primary pattern having small amplitude.

## 1 Introduction

The classical hydrodynamic problem of parametrically driven surface waves – or Faraday waves – concerns the spontaneous generation of standing waves at the free surface of a horizontal layer of fluid when subjected to vertical oscillations whose amplitude exceeds a critical value. Its usefulness as a tool to study nonlinear pattern-forming dynamics in non-equilibrium systems is reflected in the considerable amount of interest shown in the subject by experimentalists and theoreticians alike. A review of earlier works, mostly conducted with low-viscosity fluids in small vessels and a single forcing frequency, can be found in [2]. More recently, Edwards & Fauve [3] have performed experiments in the small-depth, high-viscosity and large-aspect ratio regime using a forcing function with two commensurate frequency components that modulates gravity periodically. In this regime, where it can be shown that the wavenumber of the selected pattern is less sensitive to the size and shape of the container, and that long-wavelength modes are heavily damped, observations of spatially periodic patterns (stripes, squares, hexagons), circular patterns (targets and spirals) and quasi-patterns have been reported [3,4]. A survey of more recent results has been carried out by Müller et al. [5]. Over the past two years, a new class of ‘superlattice patterns’ has been independently observed by Kudrolli et al. [1] and Arbell & Fineberg [6] in experiments employing two-frequency forcing functions, and by Wagner et al. [7] in experiments using non-Newtonian fluids. These superlattices are so termed because of their distinctive feature of having spatial structures on two different length scales when viewed at any instant in time [1]. Steady patterns that display similar characteristics have also been observed in convection experiments on fluids with temperature-dependent viscosity [8] and have been investigated in a model of long wave convection [9] and in reaction-diffusion systems near a Turing bifurcation [10].

Two types of superlattice patterns have been reported in [1] for different parameter val-

---

<sup>1</sup> Current address: Warburg Dillon Read, 100 Liverpool Street, London EC2M 2RH, UK

<sup>2</sup> E-mail: A.M.Rucklidge@damtp.cam.ac.uk

<sup>3</sup> E-mail: m-silber@northwestern.edu

ues. Both of them, despite their different spatial and spatio-temporal symmetry properties, are found to be possible transitions from harmonic standing hexagons as the forcing amplitude is increased. (In this context, *harmonic* indicates an oscillation with the same period as that of the external forcing, denoted by  $T$ , while *subharmonic* indicates an oscillation with twice that period.) The first of these patterns (called ‘superlattice-one’ by Kudrolli et al. [1]) is a harmonic response with triangular symmetry on a small scale and hexagonal lattice periodicity on a larger scale. This pattern has been studied by Silber & Proctor [11], who showed that it (along with standing hexagons) can arise in a bifurcation from the flat, undisturbed state when a hexagonal lattice with spatial periodicity larger than that dictated by the critical wavelength is considered [12,13]. Silber & Proctor [11] also suggested that stability might be transferred from standing hexagons to superlattice-one through an intermediate branch.

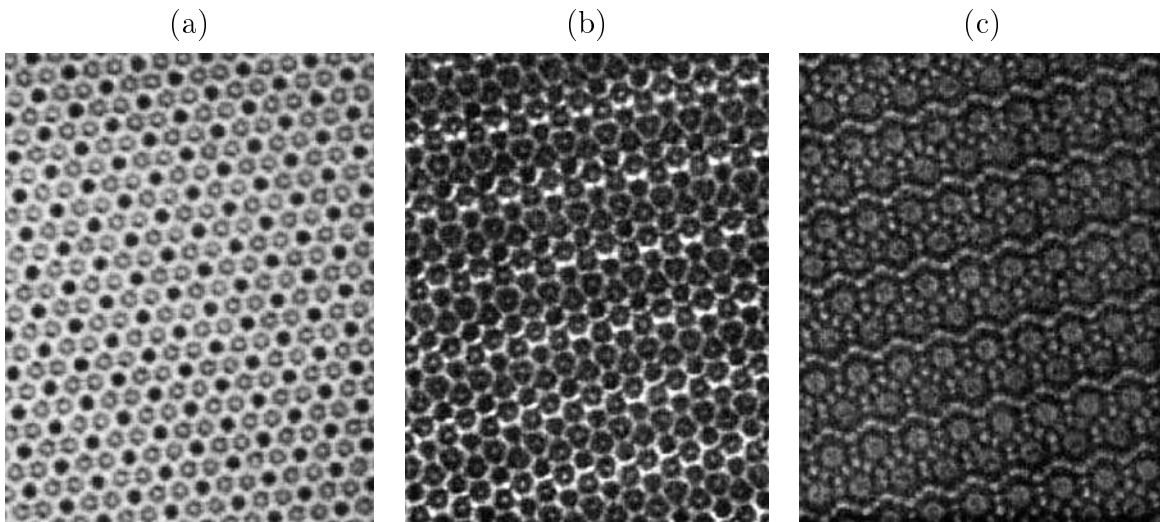


Fig. 1. (a) Time-averaged image of the superlattice-two pattern displays a well-defined hexagonal symmetry on two spatial scales. (b) & (c) Instantaneous snapshots of the same pattern separated by  $3/20$ th of the external driving period  $T$  reveals a time-dependent stripe-like modulation. The pattern in (a) is a different realization of the experiment from those in (b) & (c). Courtesy of Kudrolli et al. [1], reproduced with permission.

The second type of superlattice pattern (‘superlattice-two’ [1]), in contrast to the first, arises in a period-doubling (or subharmonic) instability of the standing hexagons. If we let  $u(\mathbf{x}, t)$  measure the deformation of the free fluid surface at time  $t$ , it satisfies

$$u(\mathbf{x}, t + 2T) = u(\mathbf{x}, t), \quad u(\mathbf{x}, t + T) \neq u(\mathbf{x}, t). \quad (1)$$

Further, this pattern exhibits a complicated mixture of spatial symmetry and time-

dependent behaviour. When averaged over two periods of the driving function, its image displays hexagonal symmetry with two well-defined spatial scales in the ratio  $1 : \sqrt{3}$  (figure 1(a)). Remarkably, at any instant, a wavy, stripe-like spatial modulation destroys the average hexagonal symmetry, resulting in a pattern that appears vastly different from its time-averaged image (see figures 1(b) and 1(c)). Arbell & Fineberg (unpublished) have also found the superlattice-two pattern for similar experimental parameters.

The superlattice-two pattern presents a number of theoretical challenges that motivate this paper: the disappearance of the stripes from the time-averaged pattern; the reduced spatial period in the time-average; and the apparent  $60^\circ$  rotation symmetry of the time-average. We present a symmetry-based approach to the study of this pattern by taking the view that it arises as a symmetry-breaking instability from the underlying standing hexagons in a spatial period-multiplying bifurcation. Our aim is to classify qualitatively the range of possible bifurcating solutions and to understand how their symmetry properties can be related to the experimental observations described above. We emphasize that we are examining instabilities of fully nonlinear states, so our approach differs from weakly nonlinear studies of the primary Faraday instability.

There are three stages in our approach. First, by using the experimentally observed instantaneous spatial symmetry information of the superlattice-two instability and by making the assumption that all solutions are periodic in the plane, we can restrict all patterns to a suitably chosen spatially periodic lattice. This lattice in turn defines a compact symmetry group, which we denote by  $\Gamma^s$ , with the key properties that its action leaves standing hexagons invariant and that it has a subgroup, which we denote by  $\Sigma^s$ , that describes the *instantaneous* spatial symmetry of the bifurcating superlattice pattern. Due to the compactness and special structure of  $\Gamma^s$ , we can compute explicitly all its irreducible representations. Second, we observe that since  $\Sigma^s$  is by definition the isotropy subgroup of the bifurcating solution under the action of  $\Gamma^s$ , it must have a non-trivial fixed-point set. This restriction allows us to identify the one relevant irreducible representation of  $\Gamma^s$  that describes the spatial symmetry properties of the marginal eigenfunctions at the superlattice bifurcation point. Finally, by considering the action of the time-shift symmetry  $\tau_t : t \rightarrow t + T$  on the period-doubling marginal modes, we obtain the irreducible representation of the full symmetry group (denoted by  $\Gamma$ ) and hence the normal form of the bifurcation problem. We can then invoke the equivariant branching lemma [14] to show that there are at least six primary branches of solutions bifurcating from standing hexagons.

With one proviso, the superlattice-two pattern observed by Kudrolli et al. [1] can be

identified as one of these branches, which we show can bifurcate as a stable branch from standing hexagons. By applying techniques for studying the averaged symmetry of periodic orbits (cf [15]), we show that the time-average of this branch of solutions has the hexagonal lattice periodicity observed in the experiment (as in figure 1(a)); this change in the spatial length scale on time-averaging is a consequence of the branch of solutions possessing a spatio-temporal symmetry. This symmetry was not reported in [1]. The proviso mentioned above is that our time-average pattern does not possess  $60^\circ$  rotation symmetry – we will return to this discrepancy in the final section.

A further stability analysis predicts that other patterns, displaying different spatial and spatio-temporal symmetry properties, can bifurcate as stable branches of solutions from standing hexagons in different regions of parameter space. More generally, our analysis indicates that patterns that display superlattice structures can arise in two-dimensional spatial period-multiplying bifurcations from an underlying non-trivial solution, and our approach could also be used to investigate other superlattice patterns of Arbell & Fineberg [6] and Wagner et al. [7]. In particular, it may be possible to analyse some of those experimental results in terms of other irreducible representations of the same group  $\Gamma^s$ .

The issue of spatial period-multiplying instabilities is an interesting one that has arisen in a variety of experimental and theoretical contexts. Period-multiplying bifurcations in one lateral direction have arisen in convection problems [16], magnetoconvection [17], Taylor–Couette experiments [18] and in numerical solutions of the Kuramoto–Sivashinsky equations [19,20]. Much less is known about spatial period-multiplying bifurcations in two directions. There are now several experimental observations of this phenomenon in the Faraday wave problem [1,6,7] as well as in convection experiments [8,16,21] and magnetoconvection calculations [22,23].

In the next section, we introduce some fundamental definitions and results from equivariant bifurcation theory [14] to help us describe how this problem can be cast into a theoretical framework. In section 3, we fully describe the symmetry group of the bifurcation problem that will give rise to the observed symmetry-breaking behaviour. We also show that, under suitable phenomenological assumptions, we can identify and hence explicitly compute the irreducible representation that is relevant to the action of the symmetry group on the observed bifurcating modes. The normal form of the bifurcation problem and a stability analysis are presented in section 4. Discussions of our approach and a comparison with the experiments follow in section 5.

## 2 Group theoretic ideas

In order to study the superlattice-two pattern as a symmetry-breaking instability from standing hexagons, it is necessary to identify all the symmetries that are initially present. Due to the apparent absence of side-wall effects in the observed patterns, we consider the mathematical idealisation that all physical fields are defined in a laterally unbounded domain. Standing hexagons are then easily seen to be invariant under the action generated by a reflection, a  $60^\circ$  rotation, and two linearly independent translations. The group generated by these symmetry actions is isomorphic to  $\mathbb{Z}^2 \dot{+} D_6$ , which is non-compact. (Here  $\mathbb{Z}$  denotes the group of integers under addition, and  $D_6$  is the twelve-element symmetry group of a regular hexagon.) Consequently a bifurcation problem that is equivariant under the action of this group can have an infinite number of modes related by symmetry becoming marginally stable simultaneously. This difficulty can be resolved if we restrict possible solutions to doubly-periodic functions defined on a suitably chosen lattice, an assumption justified by the distinct spatial periodicity of the observed patterns. A suitable lattice, which can be viewed as a finite cell with periodic boundary conditions, is one that captures the spatial periodicity of both the bifurcating modes as well as the standing hexagons. With respect to such a periodic cell, the symmetries that leave standing hexagons invariant now form a finite, and hence compact group that can be studied via representation theory. Our task therefore, is to make use of the available symmetry information taken from experimental observations to choose a lattice on which we can define a suitable spatial symmetry group  $\Gamma^s$  with the properties outlined in section 1. The idea of suitability can be made precise after we have introduced some basic group theoretic results.

Since we are considering bifurcations from a time-periodic solution, we formulate the bifurcation problem of the superlattice-two pattern, a period-doubling instability, by expanding about standing hexagons using a stroboscopic map  $\mathcal{G}$  in the manner described by Crawford & Knobloch [24] and Silber & Proctor [11]. Specifically, we are assuming that standing hexagons, a fixed point of the map  $\mathcal{G}$ , lose stability to subharmonic waves with period  $2T$  as a bifurcation parameter  $\mu$  is varied past zero. This implies that the linearised map  $D\mathcal{G}$  evaluated at the fixed point has a real eigenvalue passing through the value  $-1$  as the bifurcating waves become unstable. With the assumption that all fields are defined in a periodic cell such that symmetries of the standing hexagons are described by a compact group  $\Gamma^s$ , the linearised map  $D\mathcal{G}$  has a finite number ( $p$ ) of marginal eigenfunctions associated with the eigenvalue  $-1$  as  $\mu$  crosses zero. We denote the amplitudes of these  $p$  marginal modes at time  $t = qT$ ,  $q \in \mathbb{Z}$  by  $\mathbf{z}_q = [z_1(qT), \dots, z_p(qT)] \in \mathbb{R}^p$ .

In addition, the pattern has two neutrally stable modes (eigenvalues equal to 1) associated with translations of the standing hexagons (see [18,25]); the amplitudes of these two modes, which correspond to the translation of the pattern in the plane, are denoted by  $\mathbf{d}_q$ . Close to the onset of the period-doubling instability,  $\mathcal{G}$  can be reduced to a finite-dimensional map  $\mathbf{g}$  defined on the centre manifold spanned by these amplitudes:

$$\mathbf{z}_{q+1} = \mathbf{g}(\mathbf{z}_q; \mu), \quad \mathbf{g} : \mathbb{R}^p \times \mathbb{R} \rightarrow \mathbb{R}^p, \quad (2)$$

coupled with a map  $\mathbf{h} : \mathbb{R}^p \times \mathbb{R} \rightarrow \mathbb{R}^2$  describing how the perturbation drives translations of the pattern:

$$\mathbf{d}_{q+1} = \mathbf{d}_q + \mathbf{h}(\mathbf{z}_q; \mu). \quad (3)$$

The map  $\mathbf{g}$  is forced by symmetry to be  $\Gamma^s$ -equivariant:

$$\gamma \mathbf{g}(\mathbf{z}_q; \mu) = \mathbf{g}(\gamma \mathbf{z}_q; \mu) \quad \text{for all } \gamma \in \Gamma^s, \quad (4)$$

while the map  $\mathbf{h}$  obeys

$$N_\gamma \mathbf{h}(\mathbf{z}_q; \mu) = \mathbf{h}(\gamma \mathbf{z}_q; \mu) \quad \text{for all } \gamma \in \Gamma^s, \quad (5)$$

where  $N_\gamma$  is the  $2 \times 2$  matrix that represents how the symmetry  $\gamma$  acts on a horizontal displacement vector [25]. In terms of the marginal modes, standing hexagons correspond to the trivial state,  $\mathbf{z} = \mathbf{0}$ . When considered as a symmetry-breaking bifurcation from the underlying standing hexagons, the superlattice pattern corresponds to a non-trivial, period-two solution to the map  $\mathbf{g}$ , denoted by  $\mathbf{z}_q^*$ , whose instantaneous spatial symmetry is specified by its isotropy subgroup  $\Sigma_{\mathbf{z}_q^*}^s$ :

$$\Sigma_{\mathbf{z}_q^*}^s = \{ \sigma \in \Gamma^s : \sigma \mathbf{z}_q^* = \mathbf{z}_q^* \} \subset \Gamma^s. \quad (6)$$

In fact, this solution must lie in the fixed-point subspace of  $\Sigma_{\mathbf{z}_q^*}^s$ :

$$\text{Fix}(\Sigma_{\mathbf{z}_q^*}^s) = \{ \mathbf{z} \in \mathbb{R}^p : \sigma \mathbf{z} = \mathbf{z}, \text{ for all } \sigma \in \Sigma_{\mathbf{z}_q^*}^s \}, \quad (7)$$

which is a linear subspace of  $\mathbb{R}^p$  and invariant under  $\mathbf{g}$  [14].

Since standing hexagons do not possess spatio-temporal symmetries [26],  $\Gamma^s$ -equivariance is sufficient to determine the normal form of the map  $\mathbf{g}$  in the case of (temporal) period-preserving bifurcations. However, for period-doubling bifurcations there is an extra symmetry pertaining to the normal form, related to the time-shift action  $\tau_t : t \rightarrow t + T$  on the bifurcating modes. In this case, the normal form of the map  $\mathbf{g}$  is  $(\Gamma^s \times Z_2)$ -equivariant [27,28]. Once the full symmetry group of the normal form of  $\mathbf{g}$  is determined,

we can apply the equivariant branching lemma, which, with suitable interpretation, states that if certain non-degeneracy conditions are satisfied, there is a unique branch of bifurcating solutions for each isotropy subgroup of  $\Gamma \equiv \Gamma^s \times Z_2$  with a one-dimensional fixed-point subspace. So instead of solving for solutions of the nonlinear vector field  $\mathbf{g}$ , we can simply look for isotropy subgroups of  $\Gamma$  with this property. To apply the equivariant branching lemma, we need to know explicitly how symmetry acts on all the marginal modes, but experimental observations only provide information about the instantaneous spatial symmetry of one of these modes. We cannot infer directly from the observations the total number of marginal modes that are related by symmetry at the bifurcation point, nor the set of matrices that represent the action of the symmetry group  $\Gamma$  on the marginal modes and the map  $\mathbf{g}$ . However, this difficulty can be resolved if we make the (generic) assumption that the bifurcation is associated with an irreducible representation of the group  $\Gamma$ , and this is where the need to invoke representation theory arises.

In order to introduce the key properties of irreducible representations (irreps) and describe how they can be computed for a finite group  $\Gamma$ , we recall the following definitions [29].

- (i) A *representation* of the group  $\Gamma$  is a homomorphism  $\psi$  that maps  $\Gamma$  into a set of invertible  $n \times n$  matrices  $M_\Gamma$  acting on  $\mathbb{R}^n$  or  $\mathbb{C}^n$ , in other words

$$\psi(\gamma) = M_\gamma, \quad \gamma \in \Gamma, \quad M_\gamma \in M_\Gamma$$

such that  $\psi(\gamma_1\gamma_2) = \psi(\gamma_1)\psi(\gamma_2)$  for all  $\gamma_1, \gamma_2 \in \Gamma$ . The integer  $n$  is the *dimension* of the representation.

- (ii) Two  $n$ -dimensional representations  $M_\Gamma$  and  $N_\Gamma$  of  $\Gamma$  are called *equivalent* if there is an invertible  $n \times n$  matrix  $Q$  such that for each  $\gamma \in \Gamma$ ,

$$N_\gamma = Q^{-1}M_\gamma Q, \quad M_\gamma \in M_\Gamma, \quad N_\gamma \in N_\Gamma.$$

- (iii) A *conjugacy class* of  $\Gamma$  is a subset  $C$  of  $\Gamma$  such that  $\gamma^{-1}c\gamma \in C$ , for all  $c \in C$  and  $\gamma \in \Gamma$ .

- (iv) The *character* of an element  $\gamma \in \Gamma$  in a representation  $M_\Gamma$  is defined to be the trace of the matrix  $M_\gamma$ , and we denote this value by  $\chi_{M_\gamma}$ .

- (v) A representation of  $\Gamma$  on  $\mathbb{R}^n$  ( $\mathbb{C}^n$ ) is said to be *irreducible* if it does not leave invariant any proper subspace of  $\mathbb{R}^n$  ( $\mathbb{C}^n$ ).

Simplistically we can consider a representation as a set of  $n \times n$  nonsingular matrices that specifies the action of  $\Gamma$  on the vector space  $\mathbb{R}^n$  or  $\mathbb{C}^n$  and at the same time preserves the group structure. It is possible to show that every representation of a finite group

is equivalent to a unitary representation – one in which all matrices are unitary [29]. A simple result of definition (iv) is that the character of the identity element in a representation is always equal to the dimension  $n$  of that representation, and definitions (i), (iii) and (iv) imply that elements in the same conjugacy class have the same character. The characters of the irreps of  $\Gamma$  obey a set of rules inherited from the orthogonality theorem governing the underlying irreps [30] and for simple groups such as  $Z_2$ ,  $Z_6$  and  $D_6$ , the character tables can easily be constructed by appealing to those rules. The orthogonality theorem also implies that the number of irreps of a group is equal to the number of conjugacy classes. For finite groups with a semi-direct product structure of the form  $\Gamma = \mathcal{A} \dot{+} \mathcal{B}$  such that  $\mathcal{A}$  is a normal (or invariant) subgroup of  $\Gamma$  (that is,  $\gamma^{-1}a\gamma \in \mathcal{A}$  for every  $a \in \mathcal{A}$  and  $\gamma \in \Gamma$ ), the characters of the irreps of  $\mathcal{A}$  and  $\mathcal{B}$  form the building blocks in determining all the characters and constructing unitary irreps of the group  $\Gamma$  via a special algorithm [29].

In summary, analysis of the superlattice pattern using these group theoretic tools depends on our being able to find a spatial lattice or periodic cell on which standing hexagons and the marginal modes exhibiting the observed symmetries fit. The arrangement of the standing hexagons in the periodic cell then gives us a suitable symmetry group  $\Gamma^s$ , which has a subgroup  $\Sigma_{\mathbf{z}_q^s}^s$ , defined in (6), whose elements are determined from experimental observations. Once we have calculated all the characters of  $\Gamma^s$ , the restriction provided by the requirement that  $\Sigma_{\mathbf{z}_q^s}^s$  be the isotropy subgroup of the observed pattern enables us to isolate the one irrep that describes the action of  $\Gamma^s$  on all the marginal modes related to the observed bifurcating mode by symmetry. Indeterminacy in the choice of irreps can be avoided if we choose a unit cell that captures exactly one spatial period of the observed pattern. The details of this procedure are the subject of the next section.

### 3 Finding the symmetry group $\Gamma$ and the irrep for the superlattice-two bifurcation problem

A closer examination of images obtained from the experiment reveals that it is possible to impose a hexagonal lattice on the observed patterns, whose instantaneous spatial symmetries are depicted in figure 2. The choice of lattice is not unique as it can be shown that there are many possible candidates (for example a  $\sqrt{3} : 1$  rectangular lattice), but a hexagonal lattice is a natural choice due to the symmetry of the standing hexagons.

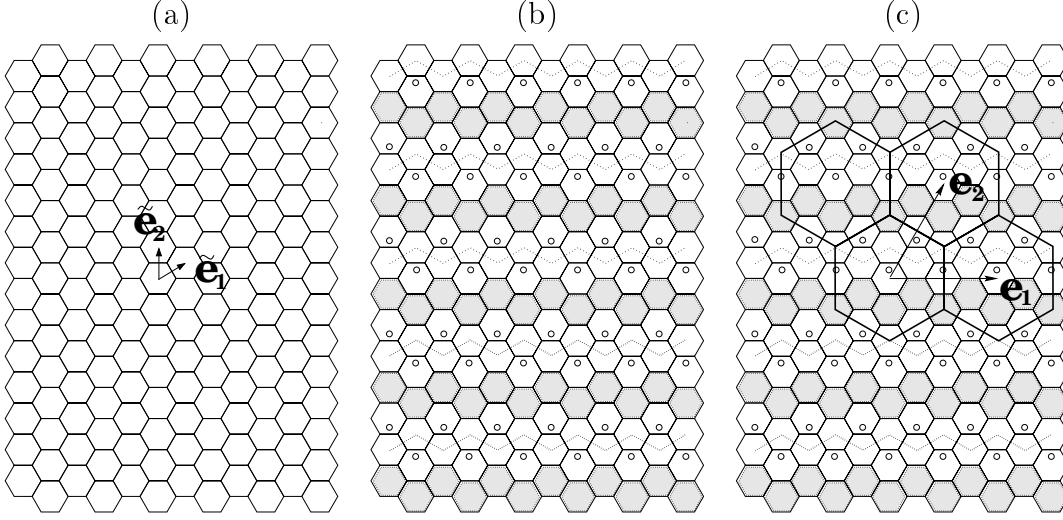


Fig. 2. (a) Schematic representation of standing hexagons, where  $\tilde{\mathbf{e}}_1$  and  $\tilde{\mathbf{e}}_2$  denote the vectors of translations defined in (10). (b) Diagram depicting the instantaneous spatial symmetry of the superlattice-two pattern (see figure 1(c)), whose spatial periodicity can be captured by hexagonal cells mapped to one another by the translations  $\mathbf{e}_1$  and  $\mathbf{e}_2$  as shown in (c). The superlattice-two pattern is left unchanged by  $\tau_2^3$ ,  $\kappa_x$  and  $\tau_1^3\rho^3$ . The small circles, dotted lines and shading in (b) and (c) serve to identify equivalent hexagons related by translations, rotations and reflections of the pattern.

Let us denote the two generating vectors of the hexagonal lattice  $\mathcal{L}$  by  $\mathbf{e}_1, \mathbf{e}_2 \in \mathbb{R}^2$  such that

$$|\mathbf{e}_1| = |\mathbf{e}_2| = c, \quad (8)$$

where  $c$  is a scaling factor (figure 2(c)). Functions in the plane that are doubly-periodic with respect to  $\mathcal{L}$  satisfy

$$u(\mathbf{x}, t) = u(\mathbf{x} + \mathbf{l}, t), \quad \mathbf{x} = (x, y) \in \mathbb{R}^2, \quad \mathbf{l} \in \mathcal{L}, \quad (9)$$

where the lattice is defined as

$$\mathcal{L} = \{n_1\mathbf{e}_1 + n_2\mathbf{e}_2 : (n_1, n_2) \in \mathbb{Z}^2\}.$$

First let us consider the spatial symmetries of the standing hexagons shown schematically in figure 2(a). They are invariant under the action of  $D_6$  as well as two translations, which we define as follows:

$$\tau_1 : \mathbf{x} \rightarrow \mathbf{x} + \tilde{\mathbf{e}}_1, \quad \tau_2 : \mathbf{x} \rightarrow \mathbf{x} + \tilde{\mathbf{e}}_2, \quad (10)$$

and let  $|\tilde{\mathbf{e}}_1| = |\tilde{\mathbf{e}}_2| = c_0$  be the observed size of the periodic cell in which the basic standing hexagons fit. Our aim is to pick a value for the scaling factor  $c$  in (8) in terms of  $c_0$ . As indicated at the end of section 2, a suitable choice of the value  $c$  is one that gives a hexagonal cell whose size captures precisely one spatial period of the bifurcating modes, as shown schematically in figure 2(c). In fact, the observed ratio of the two lengths  $|\mathbf{e}_i|$  and  $|\tilde{\mathbf{e}}_i|$  is  $c/c_0 = 2\sqrt{3}$ , and for this value of  $c$ , the symmetry group  $\Gamma^s$  of the standing hexagons includes non-trivial translations generated by  $\tau_1$  and  $\tau_2$ . The structure of the group  $\langle \tau_1, \tau_2 \rangle$  can be determined if we express each of the translations in (10) in terms of  $\mathbf{e}_1$  and  $\mathbf{e}_2$ . We can then look for the lowest powers  $n_1, n_2, n_3, n_4 \in \mathbb{Z}^+$  such that  $\tau_1^{n_1}, \tau_2^{n_2}, \tau_1^{n_3}\tau_2^{n_4}$  map the lattice  $\mathcal{L}$  to itself, and thus determine the order of the group  $\langle \tau_1, \tau_2 \rangle$ .

Guided by the experimental observations, we choose  $\tilde{\mathbf{e}}_1 = c_0 \left( \frac{\sqrt{3}}{2}, \frac{1}{2} \right)$ ,  $\tilde{\mathbf{e}}_2 = c_0 (0, 1)$  such that  $\mathbf{e}_1 = 4\tilde{\mathbf{e}}_1 - 2\tilde{\mathbf{e}}_2 = c_0(2\sqrt{3}, 0)$ ,  $\mathbf{e}_2 = 2\tilde{\mathbf{e}}_1 + 2\tilde{\mathbf{e}}_2 = c_0(\sqrt{3}, 3)$  (see figure 2). The translations can now be written as

$$\tau_1 : \mathbf{x} \rightarrow \mathbf{x} + \frac{1}{6}\mathbf{e}_1 + \frac{1}{6}\mathbf{e}_2, \quad \tau_2 : \mathbf{x} \rightarrow \mathbf{x} - \frac{1}{6}\mathbf{e}_1 + \frac{1}{3}\mathbf{e}_2, \quad (11)$$

and we can easily show that they satisfy  $\tau_1^6 = \tau_2^6 = \tau_1^2\tau_2^2 = \text{identity}$ , as vectors of the form  $\mathbf{x} + m_1\mathbf{e}_1 + m_2\mathbf{e}_2$  for any integers  $m_1$  and  $m_2$  lie in  $\mathcal{L}$  and are therefore identified. Since  $\tau_1$  and  $\tau_2$  commute we can also see that every element generated by  $\tau_1$  and  $\tau_2$  can be written as  $\tau_1^n\tau_2$  or  $\tau_1^n$  for  $n = 0, \dots, 5$ . In total there are twelve different translations, forming a group that is isomorphic to  $Z_6 \times Z_2$ . The order of this group being twelve corresponds to the fact that each of the large hexagonal cells in figure 2(c) contains exactly twelve of the smaller hexagons.

So in terms of the lattice  $\mathcal{L}$ , the full spatial symmetry of the standing hexagons is given by the group  $\Gamma^s = (Z_6 \times Z_2) \dot{+} D_6$ , where  $D_6$  is generated by a reflection  $\kappa_x$  and a  $60^\circ$  rotation  $\rho$  and its standard action on  $\mathbb{R}^2$  is given by

$$\kappa_x : (x, y) \rightarrow (-x, y), \quad \rho : (x, y) \rightarrow \frac{1}{2} \left( x - \sqrt{3}y, \sqrt{3}x + y \right), \quad (12)$$

and  $Z_6 \times Z_2$ , an invariant subgroup of  $\Gamma^s$ , is generated by the two translations

$$\tau_1 : (x, y) \rightarrow \left( x + \frac{\sqrt{3}}{2}c_0, y + \frac{1}{2}c_0 \right), \quad \tau_2 : (x, y) \rightarrow (x, y + c_0). \quad (13)$$

The group  $\Gamma^s$  has the semi-direct product structure mentioned in section 2. As a result we can apply the algorithm taken from [29] to calculate all its characters and irreps, and we present the characters of its irreps in table 1.

Irrep	Conjugacy classes of $\Gamma^s$														
	$id$	$\kappa_x$	$\rho$	$\rho\kappa_x$	$\rho^2$	$\rho^3$	$\tau_1^3\rho^3\kappa_x$	$\tau_2\rho^2$	$\tau_1^3\rho^3$	$\tau_2$	$\tau_1\kappa_x$	$\tau_2\kappa_x$	$\tau_2^3$	$\tau_1^3\kappa_x$	$\tau_1^2$
	(1)*	$\tau_2^3\kappa_x$ (6)*	(24)	(18)	(8)	(3)	$\tau_1\tau_2\rho^3\kappa_x$ (18)*	(16)	$\tau_1\tau_2\rho^3$ (9)*	(6)	(12)	(12)	(3)*	(6)	(2)
$M_{\Gamma^s}^1$	1	1	1	1	1	1	1	1	1	1	1	1	1	1	1
$M_{\Gamma^s}^2$	1	-1	1	-1	1	1	-1	1	1	1	-1	-1	1	-1	1
$M_{\Gamma^s}^3$	1	1	-1	-1	1	-1	-1	1	-1	-1	-1	-1	1	-1	1
$M_{\Gamma^s}^4$	1	-1	-1	1	1	-1	1	1	-1	1	-1	-1	1	-1	1
$M_{\Gamma^s}^5$	2	0	1	0	-1	-2	0	-1	-2	2	0	0	2	0	2
$M_{\Gamma^s}^6$	2	0	-1	0	-1	2	0	-1	2	2	0	0	2	0	2
$M_{\Gamma^s}^7$	2	2	0	0	2	0	0	-1	0	-1	-1	-1	2	2	-1
$M_{\Gamma^s}^8$	2	-2	0	0	2	0	0	-1	0	-1	1	1	2	-2	-1
$M_{\Gamma^s}^9$	3	1	0	1	0	3	-1	0	-1	-1	-1	1	-1	-1	3
$M_{\Gamma^s}^{10}$	3	-1	0	1	0	-3	-1	0	1	-1	1	-1	-1	1	3
$M_{\Gamma^s}^{11}$	3	-1	0	-1	0	3	1	0	-1	-1	1	-1	-1	1	3
$M_{\Gamma^s}^{12}$	3	1	0	-1	0	-3	1	0	1	-1	-1	1	-1	-1	3
$M_{\Gamma^s}^{13}$	4	0	0	0	-2	0	0	1	0	-2	0	0	4	0	-2
$M_{\Gamma^s}^{14}$	6	-2	0	0	0	0	0	0	0	1	-1	1	-2	2	-3
$M_{\Gamma^s}^{15}$	6	2	0	0	0	0	0	0	0	1	1	-1	-2	-2	-3

Table 1

Character table of the group of spatial symmetries  $\Gamma^s$  constructed via the algorithm taken from [29]. A representative element is shown for each conjugacy class, and the number of elements in the class is given in brackets. Classes marked by \* contain elements (specified at the top of the table) of the eight-element group  $\Sigma_{\mathbf{z}_q^s} = \langle \tau_2^3, \kappa_x, \tau_1^3\rho^3 \rangle$ .

Any elements that have the same character as the identity in a unitary irrep of  $\Gamma^s$  must also act like the identity [31]. Using this simple idea and the information taken from experimental observations about the spatial symmetries of the unstable mode, we can

single out the irrep of  $\Gamma^s$  that describes the instantaneous symmetry-breaking behaviour. Careful study of snapshots of the superlattice-two pattern shows that it is invariant under the action of  $\tau_2^3$ ,  $\kappa_x$  and  $\tau_1^3\rho^3$  (see figures 1(b) and 1(c), where the pattern is shown at a slightly tilted angle, and figure 2(b)). The group generated by these elements is by definition the isotropy subgroup of the bifurcating mode under the action of  $\Gamma^s$  (cf (6)), therefore

$$\Sigma_{\mathbf{z}_q^*}^s \equiv \langle \tau_2^3, \kappa_x, \tau_1^3\rho^3 \rangle \subset \Gamma^s. \quad (14)$$

We can now go through the list of characters of  $\Gamma^s$  given in table 1 and determine which irrep satisfies the criteria of permitting  $\Sigma_{\mathbf{z}_q^*}^s$  defined in (14) to be an isotropy subgroup of the bifurcating solution. First, any irreps that satisfy

$$\chi_{M_{\gamma_s}} = \chi_{M_{id}} \text{ for some } \gamma_s \in \Gamma^s \text{ and } \gamma_s \notin \Sigma_{\mathbf{z}_q^*}^s \quad (15)$$

must be rejected, because in these cases the isotropy subgroup of  $\mathbf{z}_q^*$  must contain spatial symmetry elements apart from those that are observed. This eliminates representations 1–12. In representation 13, the class containing  $\tau_2^3$  is represented by the identity, but this class also contains  $\tau_1^3$  and  $\tau_1\tau_2$ , which are not in  $\Sigma_{\mathbf{z}_q^*}^s$ , so eliminating this irrep and leaving only 14 and 15. Then we can use the trace formula [14] to calculate the dimension of the fixed-point subspace of  $\Sigma_{\mathbf{z}_q^*}^s$ :

$$\dim \text{Fix}(\Sigma) = \frac{1}{|\Sigma|} \sum_{\sigma \in \Sigma} \chi_{M_\sigma},$$

which gives 0 for representation 14 and 1 for representation 15. Clearly we require  $\dim \text{Fix}(\Sigma_{\mathbf{z}_q^*}^s) \neq 0$ , since  $\text{Fix}(\Sigma_{\mathbf{z}_q^*}^s)$  is non-trivial. Thus the six-dimensional irrep  $M_{\Gamma^s}^{15}$  is the only one in which  $\Sigma_{\mathbf{z}_q^*}^s$  satisfies the conditions of being an isotropy subgroup of the observed mode.

In addition to being equivariant under the action of spatial symmetries as specified by this irrep, the normal form of the period-doubling bifurcation problem has an extra symmetry corresponding to a translation in time by one period of the external forcing:

$$\tau_t : t \rightarrow t + T. \quad (16)$$

This element can be viewed as a spatio-temporal symmetry with a trivial spatial action, and it acts independently from elements in  $\Gamma^s$  with respect to the standing hexagons. So the full symmetry group  $\Gamma$  of the normal form for the superlattice bifurcation problem is a direct product between  $\Gamma^s$  and the group  $\langle \tau_t \rangle$ , which, as can be seen from (1) and (16), is isomorphic to  $Z_2$ , hence  $\Gamma = \Gamma^s \times Z_2$  as we pointed out in section 2. We can write each

element  $\gamma \in \Gamma$  as

$$\gamma = (\gamma_s, \sigma_t), \quad \gamma_s \in \Gamma^s, \quad \sigma_t \in \langle \tau_t \rangle, \quad (17)$$

such that for  $\gamma_1 = (\gamma_{s_1}, \sigma_{t_1})$ ,  $\gamma_2 = (\gamma_{s_2}, \sigma_{t_2})$ ,  $\gamma_1 \gamma_2 = (\gamma_{s_1} \gamma_{s_2}, \sigma_{t_1} \sigma_{t_2})$ . Because of the direct product structure of  $\Gamma$  and the period-doubling nature of the bifurcating solution,  $\tau_t$  must act like  $-1$  on the amplitudes of the marginal modes. Therefore the irrep of  $\Gamma$  that specifies the action of spatial and spatio-temporal symmetry elements on the marginal modes and the normal form of  $\mathbf{g}$  can be constructed from the set of matrices  $M_{\gamma_s} \in M_{\Gamma^s}^{15}$  as follows:

$$M_\gamma = \begin{cases} M_{\gamma_s} & \text{if } \sigma_t = \text{identity} \\ -M_{\gamma_s} & \text{if } \sigma_t = \tau_t \end{cases}$$

for all  $\gamma = (\gamma_s, \sigma_t) \in \Gamma$ . This irrep, which we denote by  $M_\Gamma$ , is of the same dimension as  $M_{\Gamma^s}^{15}$ , which implies that we have a six-dimensional centre manifold at the bifurcation point. So all bifurcating solutions can be written as  $u(\mathbf{x}, t) = u_0(\mathbf{x}, t) + \zeta(\mathbf{x}, t)$  such that

$$\zeta(\mathbf{x}, qT) = A_q f_1(\mathbf{x}) + B_q f_2(\mathbf{x}) + C_q f_3(\mathbf{x}) + \text{c.c.} + \text{h.o.t.}, \quad q \in \mathbb{Z} \quad (18)$$

where  $u_0(\mathbf{x}, t)$  represents standing hexagons, c.c. denotes complex conjugate, h.o.t. denotes the higher-order terms, and  $A_q, B_q, C_q \in \mathbb{C}$  are the small amplitudes of  $f_1, f_2$  and  $f_3$ , the three complex marginal eigenfunctions that form a basis for the neutral eigenspace (excluding the two zero eigenvalues corresponding to translating the underlying pattern). Note that by including the higher-order terms,  $\zeta$  represents the nonlinear perturbation from the standing hexagons.

Applying the method described in [29], we can construct all the  $6 \times 6$  matrices  $M_\gamma$  that specify the action of  $\Gamma$  on  $\mathbb{R}^6$  (or  $\mathbb{C}^3$ ) for the irrep  $M_\Gamma$ . Rather than describe this procedure, we find it convenient to specify the group action by choosing a small number of Fourier modes to represent the marginal eigenfunctions, and working out how the amplitudes of these modes  $A_q, B_q$  and  $C_q$  transform under the generating elements of  $\Gamma$ . Since representations are defined only up to a similarity transformation, the choice of Fourier modes we make will not matter, as long as we are careful not to introduce any accidental symmetries (which would become apparent on checking the characters).

Any function  $u(\mathbf{x}, t)$  defined on the lattice  $\mathcal{L}$  can be written as a double Fourier series

of the form

$$u(\mathbf{x}, t) = \sum_{j_1 \in \mathbb{Z}} \sum_{j_2 \in \mathbb{Z}} u_{j_1, j_2}(t) e^{2\pi i(j_1 \mathbf{k}_1 + j_2 \mathbf{k}_2) \cdot \mathbf{x}}, \quad (19)$$

where  $\mathbf{k}_1$  and  $\mathbf{k}_2$  are the generating wavevectors of the dual lattice  $\mathcal{L}^*$  related to  $\mathbf{e}_1$  and  $\mathbf{e}_2$  by  $\mathbf{k}_i \cdot \mathbf{e}_j = \delta_{ij}$  such that (9) holds. Our choice of the vectors  $\mathbf{e}_1$  and  $\mathbf{e}_2$  requires  $\mathbf{k}_1 = k \left( \frac{\sqrt{3}}{2}, -\frac{1}{2} \right)$ , and  $\mathbf{k}_2 = k(0, 1)$ , where  $k = \frac{1}{3c_0}$ .

We use the observed instantaneous symmetry of the pattern (see figure 2(c)) to select a representative function from the full set of Fourier modes, starting with a single Fourier mode  $e^{2\pi i(j_1 \mathbf{k}_1 + j_2 \mathbf{k}_2) \cdot \mathbf{x}}$  (and its complex conjugate) for some choice of integers  $j_1$  and  $j_2$ . If the pattern is to be invariant under  $\tau_2^3$ ,  $j_1$  must be even, so set  $j_1 = 2m$ , and, for later convenience, set  $j_2 = m + n$ , where  $m$  and  $n$  are integers. With this choice, the Fourier mode is  $e^{2\pi i k(\sqrt{3}mx + ny)}$ . The pattern is also invariant under  $\tau_1^3 \rho^3$ . Now  $\rho^3$  replaces the chosen mode by its complex conjugate, and  $\tau_1^3$  multiplies the mode by a complex number with unit modulus. Since  $\tau_1^3$  is of order two but not equal to the identity, it must act by multiplying the mode by  $-1$ . This forces  $m + n$  to be odd (and so for the observed pattern, the amplitude of the Fourier mode must be pure imaginary). The translation  $\tau_1$  must act with order 6 (otherwise the pattern would be invariant under a lesser translation in that direction), so  $3m + n \equiv 1 \pmod{6}$  or  $3m + n \equiv 5 \pmod{6}$ . The second of these is essentially the complex conjugate of the first, so we choose  $3m + n \equiv 1 \pmod{6}$ ;  $(m, n)$  could be  $(0, 1)$ ,  $(2, 1)$  or  $(1, 4)$ , for example. Finally, the reflection  $\kappa_x$  generates a new function  $e^{2\pi i k(-\sqrt{3}mx + ny)}$ , so the superlattice-two pattern can be exemplified by a mode of the form  $f_1 = e^{2\pi i k(\sqrt{3}mx + ny)} + e^{2\pi i k(-\sqrt{3}mx + ny)}$ . Sixty degree rotations of this function generate  $f_2$  and  $f_3$ , so we have:

$$f_1 = e^{2\pi i \mathbf{K}_1 \cdot \mathbf{x}} + e^{2\pi i \mathbf{K}_2 \cdot \mathbf{x}}, \quad f_2 = e^{2\pi i \mathbf{K}_3 \cdot \mathbf{x}} + e^{2\pi i \mathbf{K}_4 \cdot \mathbf{x}}, \quad f_3 = e^{2\pi i \mathbf{K}_5 \cdot \mathbf{x}} + e^{2\pi i \mathbf{K}_6 \cdot \mathbf{x}} \quad (20)$$

(the true eigenfunctions will be made up of linear combinations of such functions), where

$$\begin{aligned} \mathbf{K}_1 &= k(\sqrt{3}m, n), & \mathbf{K}_2 &= k(-\sqrt{3}m, n), \\ \mathbf{K}_3 &= \frac{k}{2} \left( \sqrt{3}(m+n), (-3m+n) \right), & \mathbf{K}_4 &= \frac{k}{2} \left( \sqrt{3}(-m+n), (3m+n) \right), \\ \mathbf{K}_5 &= \frac{k}{2} \left( \sqrt{3}(m+n), (3m-n) \right), & \mathbf{K}_6 &= \frac{k}{2} \left( \sqrt{3}(-m+n), -(3m+n) \right). \end{aligned}$$

These wavevectors have the same wavenumber  $K(m, n) = k\sqrt{3m^2 + n^2}$ , with  $m$  and  $n$  satisfying  $3m + n \equiv 1 \pmod{6}$ . With this choice of basis functions, the relevant irrep of  $\Gamma$  can be specified by the action of the generating elements of  $\Gamma$  on the amplitudes  $(A_q, B_q, C_q)$ :

$$\kappa_x : (A_q, B_q, C_q) \rightarrow (A_q, \bar{C}_q, \bar{B}_q), \quad (21)$$

$$\rho : (A_q, B_q, C_q) \rightarrow (B_q, C_q, \bar{A}_q), \quad (22)$$

$$\tau_1 : (A_q, B_q, C_q) \rightarrow (e^{\frac{i\pi}{3}} A_q, e^{\frac{i2\pi}{3}} B_q, e^{\frac{i\pi}{3}} C_q), \quad (23)$$

$$\tau_2 : (A_q, B_q, C_q) \rightarrow (e^{\frac{i2\pi}{3}} A_q, e^{\frac{i\pi}{3}} B_q, e^{-\frac{i\pi}{3}} C_q), \quad (24)$$

$$\tau_t : (A_q, B_q, C_q) \rightarrow (-A_q, -B_q, -C_q). \quad (25)$$

We include the subharmonic action of  $\tau_t$  here for completeness. The same representation could be constructed using the method described in [29].

## 4 Normal form of the bifurcation problem

We now have sufficient information to invoke the equivariant branching lemma [14] and describe the different patterns that must be formed in the instability that created the superlattice-two from standing hexagons. Before doing this, we will compute the normal form for the bifurcation since we need it to work out the stability of the various patterns. The irrep (21–25) we identified in section 3 implies that the reduced map  $\mathbf{g}$  introduced in (2) is six-dimensional, and we let  $\mathbf{z}_q = (A_q, B_q, C_q)$ ,  $q \in \mathbb{Z}$ ,  $A_q, B_q, C_q \in \mathbb{C}$ . As indicated earlier, the action of  $\tau_t$  defined in (16) is due to the subharmonic nature of the bifurcating modes with respect to the overall driving period  $T$  given in (1). If each iteration in  $\mathbf{z}_q$  corresponds to advancing in time by  $T$ , then  $\mathbf{z}_{q+2} = -\mathbf{z}_{q+1} = \mathbf{z}_q$ . Consequently,  $\mathbf{g}(\mathbf{z}_q) = \mathbf{z}_{q+1} = -\mathbf{z}_{q+2} = -\mathbf{g}(\mathbf{z}_{q+1}) = -\mathbf{g}(-\mathbf{z}_q)$  [32]. So the map  $\mathbf{g}$  will be an odd function of the amplitudes  $A_q$ ,  $B_q$  and  $C_q$ , as well as being  $\Gamma$ -equivariant. This information enables us to write down the form of  $\mathbf{g}$  including up to fifth order terms:

$$\begin{aligned} A_{q+1} = & -(1 + \mu) A_q + \alpha_1 |A_q|^2 A_q + \alpha_2 (|B_q|^2 + |C_q|^2) A_q + \beta_1 |A_q|^4 A_q \\ & + \beta_2 (|B_q|^4 + |C_q|^4) A_q + \beta_3 |A_q|^2 (|B_q|^2 + |C_q|^2) A_q + \beta_4 |B_q|^2 |C_q|^2 A_q \\ & + \beta_5 B_q^2 \bar{C}_q^2 \bar{A}_q + \nu \bar{A}_q^5, \end{aligned} \quad (26)$$

$$\begin{aligned} B_{q+1} = & -(1 + \mu) B_q + \alpha_1 |B_q|^2 B_q + \alpha_2 (|A_q|^2 + |C_q|^2) B_q + \beta_1 |B_q|^4 B_q \\ & + \beta_2 (|A_q|^4 + |C_q|^4) B_q + \beta_3 |B_q|^2 (|A_q|^2 + |C_q|^2) B_q + \beta_4 |A_q|^2 |C_q|^2 B_q \\ & + \beta_5 A_q^2 C_q^2 \bar{B}_q + \nu \bar{B}_q^5, \end{aligned} \quad (27)$$

$$\begin{aligned} C_{q+1} = & -(1 + \mu) C_q + \alpha_1 |C_q|^2 C_q + \alpha_2 (|A_q|^2 + |B_q|^2) C_q + \beta_1 |C_q|^4 C_q \\ & + \beta_2 (|A_q|^4 + |B_q|^4) C_q + \beta_3 |C_q|^2 (|A_q|^2 + |B_q|^2) C_q + \beta_4 |A_q|^2 |B_q|^2 C_q \\ & + \beta_5 \bar{A}_q^2 B_q^2 \bar{C}_q + \nu \bar{C}_q^5, \end{aligned} \quad (28)$$

where all coefficients are forced by symmetry to be real.

Apart from the  $\nu$  terms, the equations above are equivalent to the  $T^2 \rtimes D_6 \times Z_2$ -equivariant amplitude equations (truncated to the same order) that arise in the context of Boussinesq convection on a hexagonal lattice [14,33], once they are re-interpreted as amplitude equations rather than a map. The  $\nu$  terms have the effect of breaking the full  $T^2$  (two-torus) symmetry group of translations in a periodic domain to the discrete translations allowed by the underlying pattern. A natural question to ask is why we needed to work out the details of the representation before writing down these amplitude equations. The main reason is that we did not know in advance how many linearly independent marginal eigenfunctions are involved in the instability. Even if we had assumed that there were six, it has turned out that there are two six-dimensional irreps, only one of which is involved in the bifurcation. The other six-dimensional irrep is generated by taking  $f_1 = e^{2\pi ik(\sqrt{3}mx+ny)} - e^{2\pi ik(-\sqrt{3}mx+ny)}$  and (following a similar analysis) results in the same amplitude equation. Without realising this, one might conclude incorrectly that patterns that are odd under  $\kappa_x$  reflection might also be found in this instability. All the other irreps in table 1 have dimension less than six (that is, there are fewer than six independent marginal eigenfunctions), so the order of the relevant normal forms would be correspondingly less.

We also use (5) to write down the dynamics of the position  $\mathbf{d}_q$  of the underlying standing hexagons, truncated to quartic order:

$$\mathbf{d}_{q+1} = \mathbf{d}_q + \xi \operatorname{Im} \begin{bmatrix} A_q^2(\bar{C}_q^2 - B_q^2) - 2B_q^2 C_q^2 \\ -\sqrt{3}A_q^2(B_q^2 + \bar{C}_q^2) \end{bmatrix}, \quad (29)$$

where  $\xi$  is a constant.

We can show that there are six isotropy subgroups whose fixed-point subspaces are one-dimensional, so the equivariant branching lemma tells us that there are at least six primary bifurcating branches of solutions from standing hexagons, and we summarise these solutions in table 2. Elements accented by a tilde represent spatio-temporal symmetries, which, using the notation introduced in (17), can be written as  $\tilde{\tau}_1^3 = (\tau_1^3, \tau_t)$ , and similarly for  $\tilde{\tau}_2^3$  and  $\tilde{\rho}$ . The superlattice-two pattern corresponds to branch 2 of type I.

For the choice of wave integer pair  $(m, n) = (2, 1)$ , the instantaneous planforms of these six solution branches are illustrated schematically in figure 3. We can compare figures 3(e) and 3(f) with 1(b) and 1(c) and notice that the appearance of stripes at regular intervals in the grey-scale plots of solution branch 2 closely resembles the essential

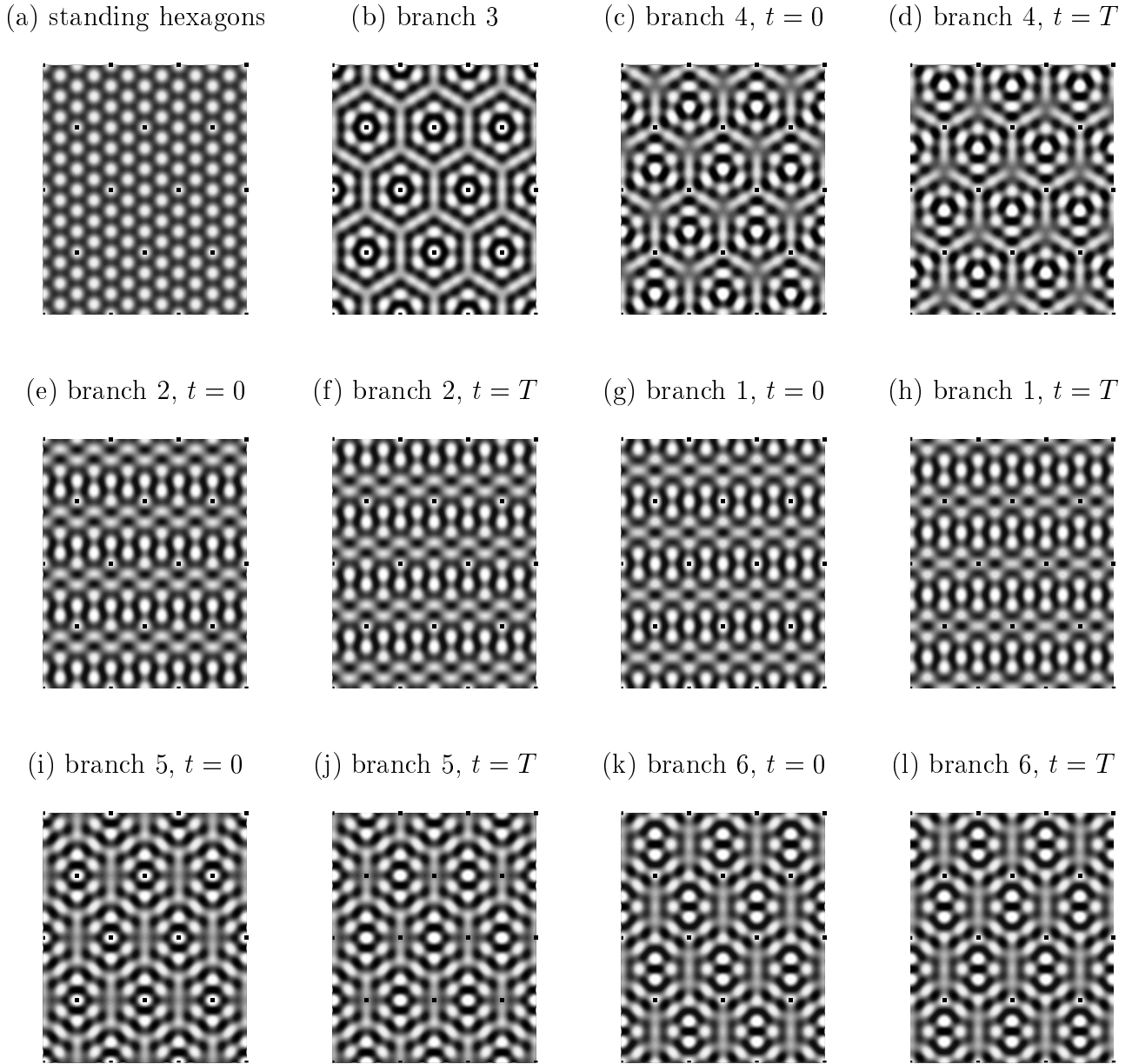


Fig. 3. Instantaneous planforms of the different solution branches summarised in table 2 and illustrated here in frames (b)–(l) as small-amplitude perturbations to standing hexagons. Solid squares represent lattice points of  $\mathcal{L}$ . (a) Standing hexagons, which have the full  $\Gamma$  symmetry. (b) Solution branch 3 with  $D_6$  symmetry, referred to in [13] as ‘superhexagons’. The periodic hexagonal boxes are delineated by light borders surrounding each cell. (c) & (d) Solution branch 4 at  $t = 0$  and  $T$  showing  $D_3$  symmetry as well as the spatio-temporal symmetry  $\tilde{\rho}$ . (e) & (f) The superlattice-two pattern corresponds to solution branch 2 as they share the same instantaneous spatial symmetries. This pattern is shown here at  $t = 0$  and  $T$  with spatio-temporal symmetry  $\tilde{\tau}_1^3$  evident. (g) & (h) Similar spatio-temporal symmetry is displayed by solution branch 1. (i)–(l) Branches 5 & 6 have very similar symmetry properties: both are invariant under the action of  $\tilde{\tau}_2^3$  and instantaneously they differ only by a shift of the reflection symmetry  $\kappa_y$ .

	representative solution branch	isotropy subgroup	averaged symmetry
I	1. $A \in \mathbb{R}, B = C = 0$	$\langle \tau_2^3, \kappa_x, \rho^3, \tilde{\tau}_1^3 \rangle$	$\langle \tau_1^3, \tau_2^3, \kappa_x, \rho^3 \rangle$
	2. $A \in i\mathbb{R}, B = C = 0$	$\langle \tau_2^3, \kappa_x, \tau_1^3 \rho^3, \tilde{\tau}_1^3 \rangle$	
II	3. $A = B = C \in \mathbb{R}$	$D_6 = \langle \kappa_x, \rho \rangle$	$D_6$
	4. $A = -B = C \in i\mathbb{R}$	$\langle \kappa_x, \tilde{\rho} \rangle$	
III	5. $A = 0, B = C \in \mathbb{R}$	$\langle \kappa_x, \rho^3, \tilde{\tau}_2^3 \rangle$	$\langle \tau_2^3, \kappa_x, \rho^3 \rangle$
	6. $A = 0, B = -C \in i\mathbb{R}$	$\langle \kappa_x, \tau_2^3 \rho^3, \tilde{\tau}_2^3 \rangle$	

Table 2

*Primary solution branches of the normal form (26–28) and their isotropy subgroups, grouped into three types, I–III. Using the analysis presented in section 4.2 we can show that the two branches within each type of solution share the same time-averaged spatial symmetries. Branch 2 of type I corresponds to the superlattice-two pattern.*

features of the experimentally observed superlattice-two pattern.

None of these primary branches leads to a net drift of the underlying hexagonal pattern; this can be seen in two ways: first, because the rate of drift (from (29), truncated to quartic order) is zero on all six primary branches; second (and more convincing) since  $\rho^3$  is in the symmetry group of all the time averaged patterns (see below). In other words, the patterns are all pinned by the  $180^\circ$  rotation symmetry on average.

#### 4.1 Stability results

We summarise in table 3 the branching equations and the Floquet multipliers of the period  $2T$  patterns, for each of the six primary solutions guaranteed to exist by the equivariant branching lemma. Floquet multipliers greater than one in magnitude indicate instability. We group the six branches into three types and denote them by I, II and III as shown in tables 2 and 3. It is evident that branches within each type are degenerate up to third-order terms, thus necessitating the inclusion of quintic terms. In particular, only one solution branch within each of types I and II can be stable depending on the signs of  $\nu$  and  $\beta_5 + \nu$ , and both branches in type III are always unstable. Only one branch can bifurcate stably, and all branches must be supercritical for one of them to be stable. One

of the requirements for the observed superlattice-two pattern (i.e., branch 2 of type I) to be stable is that the quintic coefficient  $\nu > 0$ . If we also assume the non-degeneracy conditions  $\alpha_1 \neq 0$ ,  $\alpha_1 + 2\alpha_2 \neq 0$ ,  $\alpha_1 \pm \alpha_2 \neq 0$ ,  $\nu \neq 0$  and  $\beta_3 + \nu \neq 0$ , close to the bifurcation point the relative stability of branches of the three types is illustrated by the bifurcation diagrams shown in figure 4.

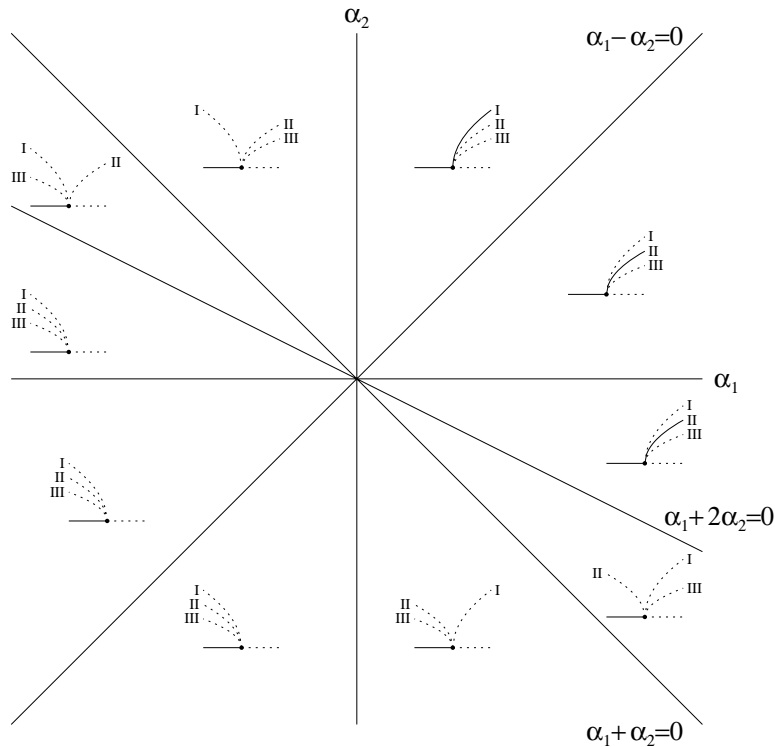


Fig. 4. Bifurcation diagrams for the  $\Gamma$ -equivariant normal form (26–28). The sign of the cubic coefficient  $\alpha_1$  determines whether solution type I bifurcates sub- or supercritically. If we assume that the quintic coefficient  $\nu > 0$ , then the superlattice-two pattern (branch 2 of type I) can occur as a stable branch in the region of the  $(\alpha_1, \alpha_2)$  space given by  $\{(\alpha_1, \alpha_2) : \alpha_1 > 0, \alpha_2 > \alpha_1\}$ .

The experimental results [1] suggest that the bifurcation may have subcritical branches as there is a parameter regime in which standing hexagons and the superlattice-two pattern may coexist. On the other hand, the experimentalists report no hysteresis between standing hexagons and superlattice-two, while they do report hysteresis between hexagons and other patterns at other parameter values, so it is not clear whether or not there is a direct bifurcation from standing hexagons to the superlattice-two pattern in the experiments. With our parameters, we require  $\alpha_1 > 0$ ,  $\alpha_2 > \alpha_1$  and  $\nu > 0$  for the superlattice-two pattern (branch 2 of type I) to bifurcate stably, but the branch could also be stable in the region  $\alpha_1 < 0$ ,  $\alpha_2 > \alpha_1$  and  $\nu > 0$  if there were a saddle-node bifurcation on branch I.

Primary solutions and branching equations		Floquet multipliers (multiplicity)
I	1. $A_q = R_1, B_q = C_q = 0,$ $0 = -\mu + \alpha_1 R_1^2 + (\beta_1 + \nu) R_1^4$	$1 - 4\alpha_1 R_1^2, 1 - 2(\alpha_2 - \alpha_1) R_1^2$ (4 times), $1 + 12\nu R_1^4$
	2. $A_q = iR_2, B_q = C_q = 0,$ $0 = -\mu + \alpha_1 R_2^2 + (\beta_1 - \nu) R_2^4$	$1 - 4\alpha_1 R_2^2, 1 - 2(\alpha_2 - \alpha_1) R_2^2$ (4 times), $1 - 12\nu R_2^4$
II	3. $A_q = B_q = C_q = R_3,$ $0 = -\mu + (\alpha_1 + 2\alpha_2) R_3^2$ $+ (\beta_1 + 2\beta_2 + 2\beta_3 + \beta_4 + \beta_5 + \nu) R_3^4$	$1 - 4(\alpha_1 + 2\alpha_2) R_3^2,$ $1 + 4(\alpha_2 - \alpha_1) R_3^2$ (2 times), $1 + 12\nu R_3^4$ (2 times), $1 + 12(\beta_5 + \nu) R_3^4$
	4. $A_q = -B_q = C_q = iR_4,$ $0 = -\mu + (\alpha_1 + 2\alpha_2) R_4^2$ $+ (\beta_1 + 2\beta_2 + 2\beta_3 + \beta_4 - \beta_5 - \nu) R_4^4$	$1 - 4(\alpha_1 + 2\alpha_2) R_4^2,$ $1 + 4(\alpha_2 - \alpha_1) R_4^2$ (2 times), $1 - 12\nu R_4^4$ (2 times), $1 - 12(\beta_5 + \nu) R_4^4$
III	5. $A_q = 0, B_q = C_q = R_5,$ $0 = -\mu + (\alpha_1 + \alpha_2) R_5^2$ $+ (\beta_1 + \beta_2 + \beta_3 + \nu) R_5^4$	$1 - 4(\alpha_1 + \alpha_2) R_5^2, 1 + 4(\alpha_2 - \alpha_1) R_5^2,$ $1 - 2(\alpha_2 - \alpha_1) R_5^2$ (2 times), $1 + 12\nu R_5^4$ (2 times)
	6. $A_q = 0, B_q = -C_q = iR_6,$ $0 = -\mu + (\alpha_1 + \alpha_2) R_6^2$ $+ (\beta_1 + \beta_2 + \beta_3 - \nu) R_6^4$	$1 - 4(\alpha_1 + \alpha_2) R_6^2, 1 + 4(\alpha_2 - \alpha_1) R_6^2,$ $1 - 2(\alpha_2 - \alpha_1) R_6^2$ (2 times), $1 - 12\nu R_6^4$ (2 times)

Table 3

*Branching equations and Floquet multipliers for the six primary period-two solutions of the normal form (26–28) listed in table 2.  $A_q, B_q$  and  $C_q$  are complex amplitudes of the marginal modes defined in (18). Only leading order terms in  $R_i$  are shown, and the multiplicities of the Floquet multipliers (computed from the second iterate of the map) are indicated.*

#### 4.2 Time-averaged behaviour

We can study the symmetry properties of the time-averaged image of the observed solution by integrating over a full period of the newly created periodic orbit (cf [15,25,34]).

Specifically, we let  $u_0(\mathbf{x}, t)$  be the standing hexagons solution and  $\zeta(\mathbf{x}, t)$  the nonlinear perturbation to this solution such that  $u(\mathbf{x}, t) = u_0(\mathbf{x}, t) + \zeta(\mathbf{x}, t)$  represents the observed pattern. We know that  $u_0(\mathbf{x}, t)$  is  $\Gamma$ -invariant, i.e.,  $\gamma u_0(\mathbf{x}, t) = u_0(\mathbf{x}, t)$  for all  $\gamma \in \Gamma$ , and have also found that the spatial and spatio-temporal symmetry of  $\zeta(\mathbf{x}, t)$  is given by its isotropy subgroup  $\langle \tau_2^3, \kappa_x, \tau_1^3 \rho^3, \tilde{\tau}_1^3 \rangle \equiv \Sigma_\zeta \subset \Gamma$ . Let  $\gamma_s$  and  $\gamma_t$  denote respectively the purely spatial symmetry elements and the spatial part of spatio-temporal symmetry elements in  $\Sigma_\zeta$  that act on  $\zeta(\mathbf{x}, t)$  as follows:

$$\gamma_s \zeta(\mathbf{x}, t) = \zeta(\mathbf{x}, t), \quad \gamma_t \zeta(\mathbf{x}, t) = \zeta(\mathbf{x}, t + T).$$

The time-averaged value of  $u(\mathbf{x}, t)$  can be obtained by integrating over the full period of the bifurcating solution:

$$\begin{aligned} \bar{u}(\mathbf{x}) &= \frac{1}{2T} \int_0^{2T} u_0(\mathbf{x}, t) + \zeta(\mathbf{x}, t) dt \\ &= \bar{u}_0(\mathbf{x}) + \frac{1}{2T} \int_0^T \zeta(\mathbf{x}, t) + \zeta(\mathbf{x}, t + T) dt, \end{aligned} \quad (30)$$

where we have used the fact that  $u_0(\mathbf{x}, t) = u_0(\mathbf{x}, t + T)$ . Clearly,  $\bar{u}$  shares the same spatial symmetry with  $\zeta$  because both  $\bar{u}_0$  and the individual entries of the integrand in (30) are invariant under the action of  $\gamma_s \in \Sigma_\zeta$ . It is also invariant under  $\gamma_t$  because the integrand in (30) as a whole is invariant under  $\gamma_t$ :

$$\begin{aligned} \gamma_t \bar{u}(\mathbf{x}) &= \gamma_t \bar{u}_0(\mathbf{x}) + \frac{1}{2T} \int_0^T \gamma_t \zeta(\mathbf{x}, t) + \gamma_t \zeta(\mathbf{x}, t + T) dt \\ &= \bar{u}_0(\mathbf{x}) + \frac{1}{2T} \int_0^T \zeta(\mathbf{x}, t + T) + \zeta(\mathbf{x}, t) dt \\ &= \bar{u}(\mathbf{x}). \end{aligned}$$

This result in fact follows readily from more general results on the symmetries of chaotic attractors [15,34].

In the case of the observed superlattice-two pattern with isotropy subgroup  $\Sigma_\zeta$ , the spatial component of the spatio-temporal symmetry element, namely  $\tau_1^3$ , will show up alongside  $\tau_2^3$ ,  $\kappa_x$  and  $\tau_1^3 \rho^3$  in the time-averaged image to generate an augmented spatial symmetry group  $\Sigma_{\bar{u}} = \langle \tau_1^3, \tau_2^3, \kappa_x, \rho^3 \rangle$ . This prediction is in agreement with experimental results (figure 1(a)) and can be understood in the following way. The action of the translations  $\tau_1$  and  $\tau_2$  on  $\bar{u}(\mathbf{x})$  is of order three since  $\tau_1^3 \bar{u}(\mathbf{x}) = \tau_2^3 \bar{u}(\mathbf{x}) = \bar{u}(\mathbf{x})$ , whereas the order of the same action on  $u(\mathbf{x})$  is six. So the averaged pattern will appear to be periodic on a lattice  $\mathcal{L}_{\text{av}}$  spanned by basis vectors  $\mathbf{e}_{\text{av}}$  such that  $|\mathbf{e}_{\text{av}}| = \frac{1}{2}|\mathbf{e}_i| = \frac{1}{2}c$ . We

have shown in section 3 that  $c_0 = \frac{c}{2\sqrt{3}}$ , it follows that  $|\mathbf{e}_{\text{av}}| = \sqrt{3}|\tilde{\mathbf{e}}_i|$ . Therefore the ratio of spatial period of the averaged pattern to that of the basic standing hexagons is  $1 : \sqrt{3}$ , which is consistent with the observation reported by [1] as shown in figure 1(a). Using the same reasoning and information from the isotropy subgroups of the primary solutions given in table 2, we therefore predict both branches in each type of solutions to have the same time-averaged symmetries.

## 5 Discussion

Starting from the observed instantaneous symmetry of the superlattice-two pattern reported in [1], we have been able to show (a) that a pattern with the same instantaneous spatial symmetry as the superlattice-two pattern can bifurcate stably from standing hexagons in a spatial period-multiplying instability; (b) that the pattern has the spatio-temporal symmetry (not reported in [1]) of advancing one driving period in time combined with a translation by three units in space (figure 3(e) and 3(f)); and (c) that this spatio-temporal symmetry accounts for the intermediate spatial scale and periodicity on a hexagonal lattice of the time-averaged pattern (figure 1(a)). We should emphasise that the intermediate spatial periodicity of the time-averaged pattern is not the spatial periodicity of the larger hexagonal lattice that we have assumed.

Arbell & Fineberg (unpublished) have found the superlattice-two state in their experiments and have confirmed that it does have the spatio-temporal symmetry that we predict. Our results also suggest that  $60^\circ$  rotations are not in fact symmetries of the time-averaged pattern, but should be weakly broken. The breaking of  $60^\circ$  rotational symmetry, if it is present, is evidently a small effect since the hexagons in figure 1(a) do appear to be invariant under  $60^\circ$  rotations [1] (this has been confirmed by Gollub, private communication). For other parameter values, the symmetry breaking effect may be more pronounced: Fineberg (private communication) reports that his experimental time-averaged pattern is not invariant under  $60^\circ$  rotations. Clearly this would be an interesting issue to investigate in more detail, but the measurements are delicate and are liable to be prone to systematic errors or imperfections, so confirming our prediction could be difficult.

The spatio-temporal symmetry of superlattice-two arises because the instability of standing hexagons is subharmonic. Other patterns, with different combinations of spatial and spatio-temporal symmetries, are possible stable branches in the same bifurcation prob-

lem. Not all branches of solutions have spatio-temporal symmetries, and some of the patterns share the same time-averaged symmetries even though they have different instantaneous planforms. The method we have presented is based entirely on symmetry arguments and is able to deal with instabilities of a fully nonlinear time-periodic solution.

Spatial period-multiplying instabilities have arisen in a variety of contexts, in both one [17–20] and two lateral directions [1,6–8,16,21–23]. Most of these situations involved relatively simple groups; part of the difficulty and interest here has been the size of the symmetry group, enlarged because of the number of translations broken by the new pattern. Only one of the 15 representations is involved in the superlattice-two bifurcation; other representations may be relevant to other experiments (particularly [6,7]) in which standing hexagons lose stability to patterns that fit into the larger hexagonal cells we have used here.

As can be seen in section 3, a heuristic step in our method involves the choice of a suitable periodic cell that accommodates the observed patterns and whose size coincides with exactly one spatial period of the bifurcating modes. The arrangement of the underlying basic state in this cell then defines a spatial symmetry group  $\Gamma^s$  of the bifurcation problem and the instantaneous symmetries of the superlattice instability form its isotropy subgroup  $\Sigma^s$ . If a larger hexagonal periodic cell that captures more than one spatial period of the bifurcating modes had been chosen, the translations  $\tau_1$  and  $\tau_2$  given in (10) that leave standing hexagons invariant would have had higher order, resulting in a larger spatial symmetry group. In this case there would have been more than one irrep of  $\Gamma^s$  in which  $\Sigma^s$  satisfied the conditions of being an isotropy subgroup. By choosing the smallest possible periodic cell, we have found that such indeterminacy can be avoided.

The method we have described in this paper for analysing certain types of symmetry-breaking instabilities bifurcating from a non-trivial basic state is based entirely on the observed spatial symmetries of these patterns. However, information on spatial symmetries of the new pattern alone may not be sufficient for our approach to be applicable in some problems. For example, consider a bifurcation problem defined on a spherical domain. Suppose a basic state with  $O(3)$  symmetry loses stability and the observed bifurcating solutions are axisymmetric, then the isotropy subgroup of the bifurcating modes is given by  $O(2)$ . If the eigenfunctions are expanded in spherical harmonics, it is known that  $O(2)$  is a maximal isotropy subgroup of  $O(3)$  for *all* even values of the spherical harmonic index  $l$  [14] and so an infinite number of irreps is relevant to the observed bifurcation. This example illustrates the fact that our method breaks down if the observed symmetries of the bifurcating modes form an isotropy subgroup for more

than one irrep of the symmetry group of the basic state.

We are currently involved in applying a similar method to the study of the ‘superlattice-one’ pattern reported in [1] as a bifurcating instability from standing hexagons. Preliminary analysis of the experimental data reveals that a suitable periodic box in this case will give rise to an arrangement of standing hexagons with a ‘hidden’ reflection symmetry [13], which leads to extra complications in determining the spatial symmetry group. It is an interesting problem that deserves further investigation.

Unlike some time-periodic solutions (for example, standing rolls), which can also be defined on a hexagonal lattice, standing hexagons possess only trivial spatio-temporal symmetries [26]. So our treatment of the superlattice patterns as symmetry-breaking instabilities from standing hexagons is relatively simple because only instantaneous spatial symmetries are needed to define the isotropy subgroup of these solutions. In general, our approach can be applied to the study of spatial period-multiplying bifurcations from solutions with spatio-temporal symmetries and used to investigate some of the possible symmetry-breaking behaviour, if techniques discussed by Rucklidge & Silber [25] and Lamb & Melbourne [28] are also included.

## Acknowledgements

We would like to thank Jerry Gollub for inspiring this work, Jonathan Dawes, Marty Golubitsky, Paul Matthews and Michael Proctor for sharing their insights with us, and Jay Fineberg for showing us his unpublished experimental results. DPT is grateful to the Croucher Foundation for financial support. The research of AMR is supported by EPSRC. The research of RBH was supported by King’s College, Cambridge. The research of MS is supported by NSF grant DMS-9972059, NSF CAREER award DMS-9502266, and by NASA grant NAG3-2364.

## References

- [1] A. Kudrolli, B. Pier, and J.P. Gollub, “Superlattice patterns in surface waves”, *Physica D* **123**, 99 (1998).
- [2] J. Miles and D. Henderson, “Parametrically forced surface waves”, *Annu. Rev. Fluid Mech.* **22**, 143 (1990).

- [3] W.S. Edwards and S. Fauve, “Patterns and quasi-patterns in the Faraday experiment”, *J. Fluid Mech.* **278**, 123 (1994).
- [4] A. Kudrolli and J.P. Gollub, “Patterns and spatiotemporal chaos in parametrically forced surface waves: a systematic survey at large aspect ratio”, *Physica D* **97**, 133 (1996).
- [5] H.W. Müller, R. Friedrich, and D. Papathanassiou, “Theoretical and experimental investigations of the Faraday instability”, in *Evolution of Spontaneous Structures in Dissipative Continuous Systems*, edited by F.H. Busse and S.C. Müller (Springer, Berlin, 1998), pp. 230–265.
- [6] H. Arbell and J. Fineberg, “Spatial and temporal dynamics of two interacting modes in parametrically driven surface waves”, *Phys. Rev. Lett.* **81**, 4384 (1998).
- [7] C. Wagner, H.W. Müller, and K. Knorr, “Faraday waves on a viscoelastic liquid”, *Phys. Rev. Lett.* **83**, 308 (1998).
- [8] D.B. White, “The planforms and onset of convection with a temperature-dependent viscosity”, *J. Fluid Mech.* **191**, 247 (1988).
- [9] A.C. Skeldon and M. Silber, “New stability results for patterns in a model of long-wavelength convection”, *Physica D* **122**, 117 (1998).
- [10] S.L. Judd and M. Silber, “Simple and superlattice Turing patterns in reaction-diffusion systems: bifurcation, bistability, and parameter collapse”, *Physica D* **136**, 45 (2000).
- [11] M. Silber and M.R.E. Proctor, “Nonlinear competition between small and large hexagonal patterns”, *Phys. Rev. Lett.* **81**, 2450 (1998).
- [12] B. Dionne and M. Golubitsky, “Planforms in two and three dimensions”, *Z. angew Math. Phys.* **43**, 36 (1992).
- [13] B. Dionne, A.C. Skeldon, and M. Silber, “Stability results for steady, spatially-periodic planforms”, *Nonlinearity* **10**, 321 (1997).
- [14] M. Golubitsky, I. Stewart, and D.G. Schaeffer, “Singularities and Groups in Bifurcation Theory”, (Springer, New York, 1988), Vol. 2.
- [15] E. Barany, M. Dellnitz, and M. Golubitsky, “Detecting the symmetry of attractors”, *Physica D* **67**, 66 (1993).
- [16] D. McKenzie, “The symmetry of convective transitions in space and time”, *J. Fluid Mech.* **191**, 287 (1988).
- [17] M.R.E. Proctor and N.O. Weiss, “Symmetries of time-dependent magnetoconvection”, *Geophys. Astrophys. Fluid Dynamics* **70**, 137 (1993).

- [18] G. Iooss, “Secondary instabilities of Taylor vortices into wavy inflow or outflow boundaries”, *J. Fluid Mech.* **173**, 273 (1986).
- [19] P.J. Aston, A. Spence, and W. Wu, “Bifurcation to rotating waves in equations with  $O(2)$ -symmetry”, *SIAM J. Appl. Math.* **52**, 792 (1992).
- [20] F. Amdjadi, P.J. Aston, and P. Plecháč, “Symmetry breaking Hopf bifurcations in equations with  $O(2)$  symmetry with application to the Kuramoto–Sivashinsky equation”, *J. Comp. Phys.* **131**, 181 (1997).
- [21] M.R.E. Proctor and P.C. Matthews, “ $\sqrt{2} : 1$  Resonance in non-Boussinesq convection”, *Physica D* **97**, 229 (1996).
- [22] J.H.P. Dawes, “The  $1 : \sqrt{2}$  Hopf/steady-state mode interaction in three-dimensional magnetoconvection”, *Physica D* **139**, 109 (2000).
- [23] A.M. Rucklidge, N.O. Weiss, D.P. Brownjohn, P.C. Matthews, and M.R.E. Proctor, “Compressible magnetoconvection in three dimensions: pattern formation in a strongly stratified layer”, Submitted to *J. Fluid Mech.* (2000).
- [24] J.D. Crawford and E. Knobloch, “Symmetry and symmetry-breaking bifurcations in fluid dynamics”, *Annu. Rev. Fluid Mech.* **23**, 341 (1991).
- [25] A.M. Rucklidge and M. Silber, “Bifurcations of periodic orbits with spatio-temporal symmetries”, *Nonlinearity* **11**, 1435 (1998).
- [26] M. Roberts, J.W. Swift, and D.H. Wagner, “The Hopf bifurcation on a hexagonal lattice”, *Contemp. Math.* **56**, 283 (1986).
- [27] P. Chossat and M. Golubitsky, “Iterates of maps with symmetry”, *SIAM J. Math. Anal.* **19**, 1259 (1988).
- [28] J.S.W. Lamb and I. Melbourne, “Bifurcation from periodic solutions with spatiotemporal symmetry”, in *Pattern Formation in Continuous and Coupled Systems*, edited by M. Golubitsky, D. Luss, and S.H. Strogatz (Springer, New York, 1999), pp. 175–192.
- [29] J.F. Cornwell, “Group Theory in Physics”, (Academic Press, San Diego, 1984).
- [30] K.F. Riley, M.P. Hobson, and S.J. Bence, “Mathematical Methods for Physics and Engineering”, (Cambridge University Press, Cambridge, 1998).
- [31] M.J. Collins, “Representations and Characters of Finite Groups”, (Cambridge University Press, Cambridge, 1990).
- [32] C. Elphick, E. Tirapegui, M.E. Brachet, P. Coullet, and G. Iooss, “A simple global characterization for normal forms of singular vector-fields”, *Physica D* **29**, 95 (1987).

- [33] M. Golubitsky, J.W. Swift, and E. Knobloch, “Symmetries and pattern selection in Rayleigh–Bénard convection”, *Physica D* **10**, 249 (1984).
- [34] M. Dellnitz, M. Golubitsky, and M. Nicol, “Symmetry of attractors and the Karhunen–Loeve decomposition”, in *Trends and Perspectives in Applied Mathematics*, edited by L. Sirovich (Springer, New York, 1994), pp. 73–108.